

Supporting Information

for

An Unusual OFF-ON Fluorescence Sensor for Detecting Mercury Ions in Aqueous Media and Living Cell

**Maozhong Tian,^{*a,b} Libing Liu,^a Yongjun Li,^a Ruifeng Hu,^a Taifeng Liu,^a Huibiao Liu,^a
Shu Wang,^a Yuliang Li^{*a}**

^a Beijing National Laboratory for Molecular Science, Key Laboratory of Organic Solids, Institute
of Chemistry, Chinese Academy of Sciences, Beijing 100190, P. R. China

^b College of Chemistry and Environmental Engineering, Shanxi Datong University, Datong
037009, P. R. China

Contents:

1. Materials and general methods
2. Determination of fluorescence quantum yields
3. Synthesis of sensor **BDAA**
4. Water solubility of the sensor.
5. Excitation and Emission Spectra of free sensor **BDAA** and **BDAA/Hg²⁺**
6. Crystal structure determination of **BDAA**
7. pH titration of free sensor **BDAA** and **BDAA/Hg²⁺**
8. Color changes and fluorescence changes of **BDAA** with **Hg²⁺**
9. Emission Spectra of the **BDAA/Hg²⁺** in different solvents
10. Calculated spatial distributions of HOMO and LUMO for **BDAA**
11. Fluorescence enhancement with low concentration of **Hg²⁺**
12. Calculation of apparent association constant from fluorescence studies
13. The reversibility of the sensor
14. ¹H NMR titration spectra
15. 2D H-C¹³C NMR spectra of the **BDAA** and **BDAA/Hg²⁺**
16. Infrared spectra of the **BDAA** and **BDAA+Hg²⁺**
17. MALDI-TOF mass spectrum of the **BDAA/Hg²⁺** complex
18. Interfere of anions
19. Confocal fluorescence images of live HT-29 cells with **Hg²⁺**
20. The characterization data of sensor **BDAA**
21. References

1. Materials and general methods

All the solvents were of analytic grade. The salts used in stock solutions of metal ions were $\text{Pb}(\text{NO}_3)_2$, $\text{Zn}(\text{NO}_3)_2 \cdot 6\text{H}_2\text{O}$, $\text{Ni}(\text{NO}_3)_2 \cdot 6\text{H}_2\text{O}$, $\text{Mg}(\text{NO}_3)_2 \cdot 6\text{H}_2\text{O}$, $\text{Co}(\text{NO}_3)_2 \cdot 6\text{H}_2\text{O}$, $\text{Cu}(\text{NO}_3)_2 \cdot 3\text{H}_2\text{O}$, $\text{Cd}(\text{NO}_3)_2 \cdot 4\text{H}_2\text{O}$, $\text{Cr}(\text{NO}_3)_3 \cdot 9\text{H}_2\text{O}$, $\text{Ca}(\text{NO}_3)_2 \cdot 4\text{H}_2\text{O}$, NaNO_3 , KNO_3 , AgNO_3 , $\text{Ba}(\text{NO}_3)_2$, $\text{Al}(\text{NO}_3)_3 \cdot 9\text{H}_2\text{O}$, $\text{Fe}(\text{NO}_3)_3 \cdot 9\text{H}_2\text{O}$, $\text{Hg}(\text{ClO}_4)_2 \cdot 3\text{H}_2\text{O}$. ^1H -NMR and ^{13}C -NMR spectra were measured on a BrukerARX400 spectrometer by using tetramethylsilane (TMS) as the internal standard, and chemical shifts (δ) were given in ppm relative to TMS. Matrix-assisted laser desorption/ionization reflectron time-of-flight (MALDI-TOF) mass spectrometry was performed with a BrukerBiflex III mass spectrometer. Elemental analyses were carried out with a Carlo Erba 1106 elemental analyzer. Fluorescence excitation and emission spectra were recorded by using a JASCO FP6600 spectrophotometer in a quartz cell. Electronic absorption spectra were measured on a JASCO V-579 spectrophotometer in a quartz cell. The cells were imaged by a confocal laser scanning biological microscope (FV1000-IX81, Olympus, Japan). The crystal data collection of **BDAA** was performed on a CrysAlisPro diffractometer.

Cell lines and materials: HT-29 cell lines was purchased from cell culture center of Institute of Basic Medical Sciences, CAMS and cultured in Dulbecco's Modified Eagle's Medium, High Glucose (DMEM)/Ham's F12 (vol/vol=1:1) supplemented with 5% fetal calf serum.

Cell Culture: HT-29 cells were routinely cultured in DMEM (high glucose)/Ham's F12 medium containing 10% serum and harvested for subculture using trypsin (0.05%, Gibco/Invitrogen) and grown in a humidified atmosphere containing 5% CO_2 and 95% air at 37°C . Before experiment, the cells were pre-cultured until confluence was reached.

The experiment detail to prepare the sensor solution: All spectroscopic measurements were

performed in HEPES buffer solution (50 mM, pH = 7.4). Stock solutions (5.0×10^{-2} M) of metal ions (metal nitrate, perchlorate for Hg^{2+}) were prepared in two-distilled water. The stock solution of 1.0×10^{-2} M the sensor **BDAA** was prepared in DMSO. In titration experiments, each time 3 mL aqueous solution containing 3 μL solution of **BDAA** (1.0×10^{-2} M) was filled in a quartz optical cell of 1 cm optical path length. Then various amount of $\text{Hg}(\text{II})$ stock solution was added to the compound solution with micro-pipet. Spectral data was recorded at 2 min after the addition. In selectivity experiment, the test samples were prepared by placing appropriate amounts of metal ion stock solution into 3 mL aqueous solution of **BDAA** (10 μM). For fluorescence measurements, excitation wavelength is at 430 nm.

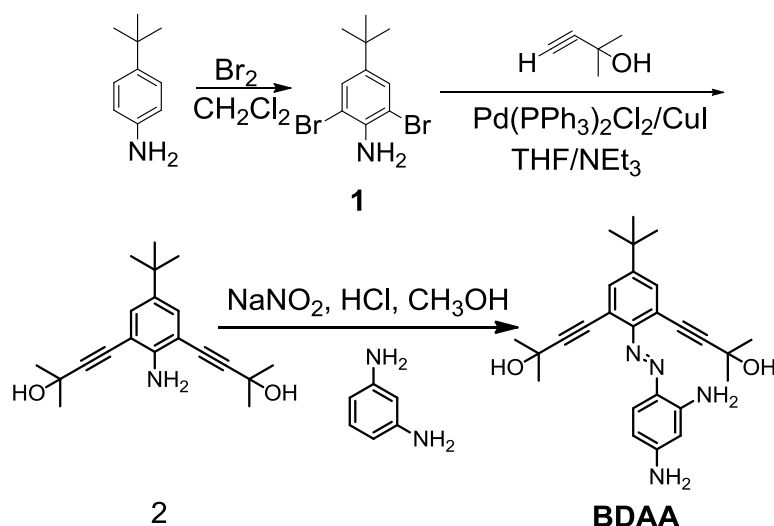
2. Determination of fluorescence quantum yields

The fluorescence efficiency of the sensor was estimated by measuring their fluorescence quantum yield using Equation (1) on the basis of the absorption and fluorescence spectra taken in the solvent. Fluorescein ($\Phi = 0.90$) in 0.1 N NaOH was used as a standard.¹

$$\Phi_{\text{sample}} = \Phi_{\text{st}} \frac{S_{\text{u}} \lambda_{\text{st}} n_{\text{Du}}^2}{S_{\text{st}} \lambda_{\text{u}} n_{\text{Dst}}^2} \quad (1)$$

Where Φ_{st} the emission quantum yield of the standard, λ_{st} and λ_{u} represent the absorbance of the standard and sample at the excited wavelength, respectively, while S_{st} and S_{u} are the integrated emission band areas of the standard and sample, respectively, and n_{Dst} and n_{Du} are the solvent refractive index of the standard and sample, u and s refer the unknown and standard, respectively.

3. Synthesis of sensor BDAA



2,6-Dibromo-4-*tert*-butylaniline (1). To a stirred solution of *p*-*tert*-butylaniline (10 g) dissolved in dichloromethane (100 mL) was added a solution of bromine (26.85 g, 167.8mmol) in 50 mL of dichloromethane dropwise via pressure addition funnel under nitrogen at room temperature. The mixture was stirred for 2 h and monitored by TLC. Evaporation of the solvent afforded a residue which was added to 20% aqueous sodium hydroxide (100 mL). The product was extracted with diethyl ether (200mL) and dried over magnesium sulfate. Filtration and evaporation of the solvent afforded a purple oil which was purified by Flash column chromatography on silica gel eluted with [Petroleum ether/ $\text{CH}_2\text{Cl}_2=5:1$ (v/v)] to provide 25.9 g (85%) of **1** as a white solid. All physical data agreed with reported literature values.²

2,6-Bis(3-methyl-3-hydroxy-1-butynyl)-4-*tert*-butylaniline (2) To a mixture of **1**(3.05 g, 10.0 mmol), $\text{PdCl}_2(\text{PPh}_3)_2$ (79.5 mg, 0.114mmol), CuI (41.9 mg, 0.221mmol) under an argon atmosphere were added Et_3N (35 mL) and then 2-methylbut-3-yn-2-ol(1.93 g, 23mmol) in Et_3N (15 mL). The resulting mixture was stirred at 50°C for 60 h. After the solution was cooled to room temperature, ethyl acetate was added to the reaction mixture, which was filtered. After evaporation of the filtrate, the residue was partitioned between CHCl_3 and H_2O , where the aqueous layer was neutralized with diluted HCl. The organic layer was washed with H_2O and brine and dried over

Na₂SO₄. After evaporation of solvent, the residue was subjected to Flashcolumn chromatography on silica gel eluted with [hexanes/EtOAc=2:1 to 1:1 (v/v)] afforded **2** as a white solid (2.61 g, 8.34 mmol, 83%). All physical data agreed with reported literature values.³

4-[(2,6-Bis(3-methyl-3-hydroxyl-1-butynyl)-4-tert-butylphenyl)azo]-1,3-benzenediamine

(BDAA). To a stirred MeOH solution (5 mL) of 2,6-Bis(3-methyl-3-hydroxyl-1-butynyl)-4-tert-butylaniline (0.313 g, 1mmol) was added slowly conc. HCl (2.5 mL). The reaction mixture was kept at 0 °. An aqueous solution (1 mL) of NaNO₂ (75.9mg, 1.1 mmol) was added dropwise to generate the azonium intermediate, and the reaction mixture was stirred for 10 min. A solution of m-phenylenediamine (0.130 g, 1.2 mmol) and sodium hydroxide (0.150 g) in MeOH–H₂O (2:1, v/v; 9 mL) was kept at 0 °C. With stirring, the azonium intermediate was added dropwise to the m-phenylenediamine solution while maintaining the temperature of the reaction at 0 °C. After stirring for 30 min, water (50 mL) was added to induce precipitation of a red solid, which was isolated by filtration and washed thoroughly with water, and dried. Flash column chromatography on SiO₂ (hexane: EtOAc = 2:1, v/v) furnished compound **BDAA** (391.5 mg, 0.906 mmol, yield = 91%).¹H NMR (400 MHz, DMSO-*d*₆, 298 K): δ 7.40, 7.38 (d, *J* = 8.8 Hz, 1H), 7.35 (s, 2H), 5.99 (m, 3H), 5.86 (d, *J* = 2.0 Hz, 1H), 5.34 (s, 2H), 1.41 (s, 12H), 1.28 (s, 9H).¹³C NMR (100 MHz, CD₃OD, 298 K) δ 154.88, 154.73, 150.31, 147.21, 133.93, 132.11, 131.84, 117.08, 107.40, 99.10, 98.42, 81.47, 66.16, 35.34, 31.86, 31.58. FT-IR (thin film on KCl, cm⁻¹): 3548, 3465, 3368, 2970, 2935, 2869, 1630, 1584, 1546, 1502, 1476, 1448, 1400, 1374, 1329, 1280, 1250, 1185, 1158, 1141, 945, 886, 820, 652, 579, 567, 452. MALDI-TOF Calcd for C₂₆H₃₂N₄O₂ [M+H]⁺ 433.25; Found 433.17. Anal. Calcd for C₂₆H₃₂N₄O₂: C, 72.19; H, 7.46; N, 12.95. Found: C, 72.27; H, 7.46; N, 12.99.

4. Water solubility of the sensor.

Small amount of dye was dissolved in DMSO to prepare the stock solutions (30 mM). The solution was diluted and added to a cuvette containing 3.0 mL of H₂O by using a micro syringe. In all cases, the concentration of DMSO in H₂O was maintained to be 0.2 %. The plots of absorbance against the dye concentration were linear at low concentration and showed downward curvature at higher concentration (Figure S2). A linear relationship between the concentration and the absorbance indicated no intermolecular association under this condition. The maximum concentration in the linear region was taken as the solubility. The solubilities of the sensor **BDAA** in water were 25 μM at least.

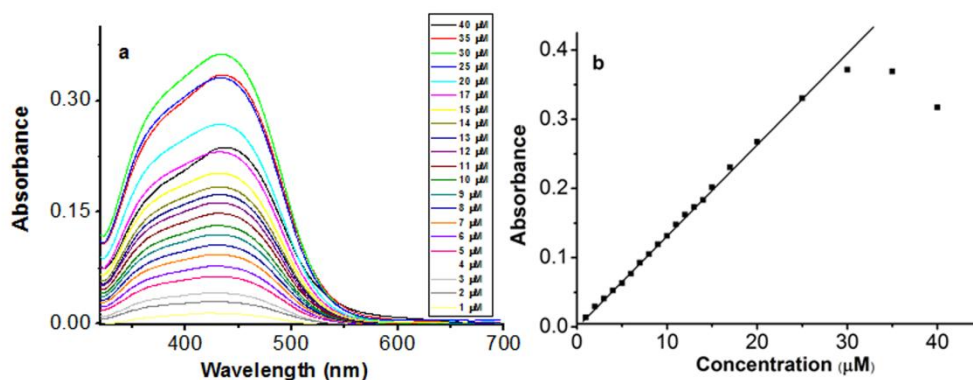


Figure S1. (a) Absorption spectra; (b) plot of absorbance against dye concentration for BDAA in H₂O.

5. Excitation and Emission Spectra of free sensor **BDAA** and **BDAA/Hg²⁺**

Solutions of compound **BDAA** (1×10^{-5} M) were prepared with 50 mM of HEPES buffer solution (0.1M KNO₃; pH=7.4). Excitation and emission spectra of compound **BDAA** before and after addition of **Hg²⁺** at room temperature in aqueous solution were measured.

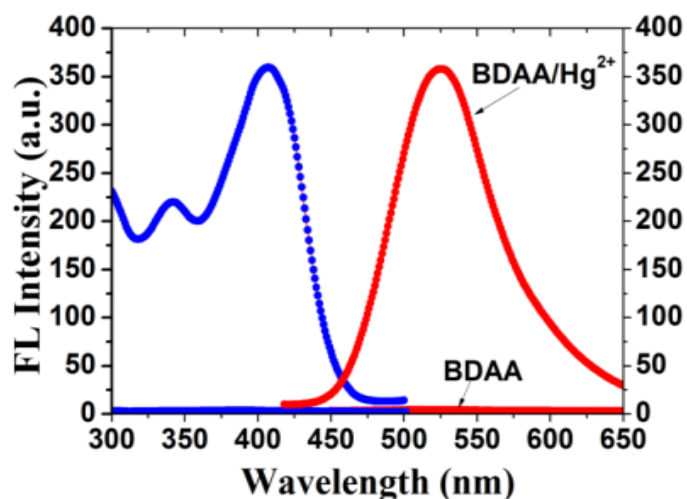


Figure S2. Excitation and emission spectra of free sensor **BDAA** and **BDAA/Hg²⁺** in HEPES buffer solution (50 mM, pH = 7.4). Excitation and emission slit widths were 3 and 6 nm, respectively.

6. Crystal structure determination of **BDAA**.

Red crystals of **BDAA** were grown upon EtOAc/Hexane mixture solution at 25 °C. The data collection of **BDAA** was performed on a CrysAlisPro diffractometer using mirror monochromated Cu-K_α radiation ($\lambda = 1.5418 \text{ \AA}$). Intensities were measured by ω -scans and corrected for background, polarization and Lorentz effects. A semi-empirical absorption correction was applied for the data sets. The structure was solved by direct methods and refined anisotropically by the least-squares procedure implemented in the SHELX program system.⁴

Table S1. Selected Crystallographic and Data Collection Parameters for sensor **BDAA**

empirical formula	C ₂₆ H ₃₂ N ₄ O ₂
formula weight	432.56
crystal system	triclinic
space group	$P\bar{1}$
a (Å)	11.7693(5)
b (Å)	19.6839(10)
c (Å)	22.7064(7)
α (deg)	112.090(4)
β (deg)	90.068(3)
γ (deg)	99.006(4)
volume (Å ³)	4803.7(3)
Z	8
density (calcd) (g · cm ⁻³)	1.196
absorption coeff (mm ⁻¹)	0.609
F(000)	1856
crystal color and shape	Red and needle
θ range for data collection	3.80°–63.69°
reflections collected	23886
independent reflections	23886
observed reflections [$I > 2\sigma(I)$]	15961
data/restraints/parameters	23886/0/1190
goodness-of-fit on F^2	1.086
final R indices [$I > 2\sigma(I)$]	$R_1 = 0.0749$, $wR_2 = 0.2076$
R indices (all data)	$R_1 = 0.1106$, $wR_2 = 0.2388$
Largest diff. peak and hole (e · Å ⁻³)	0.530 and -0.489

7. pH titration of free sensor BDAA and BDAA/Hg²⁺

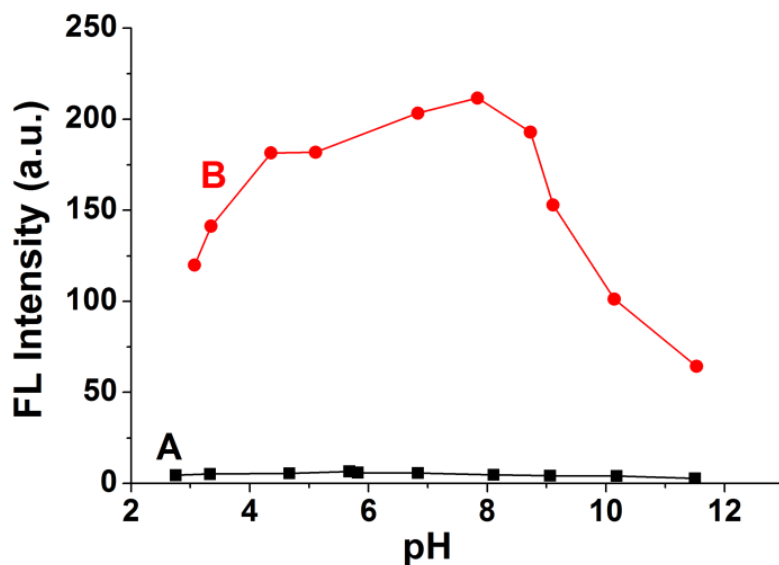


Figure S3. Fluorescence intensity (525 nm) of free **BDAA** (10 μM) (A) and after addition of 30 μM of Hg^{2+} (B) in 50 mM of HEPES buffer solution (pH = 7.4) as a function of different pH values. Excitation at 430 nm.

8. Colorimetric changes and fluorescence changes of BDAA with Hg²⁺

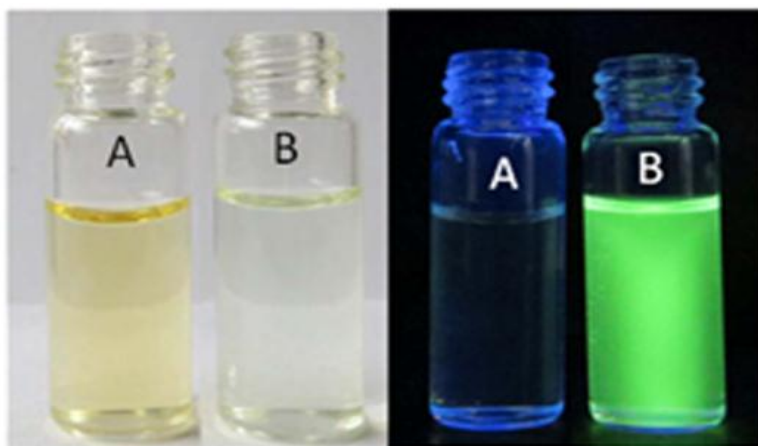


Figure S4. Visual colorimetric change (left) and fluorescence change (right) of **BDAA** (10 μM) observed in HEPES buffer (50 mM, containing 0.1M KNO_3 , pH=7.4) solution after addition of 3 equiv Hg^{2+} (A: free **BDAA**; B: **BDAA**+ Hg^{2+}).

9. Emission Spectra of BDAA/Hg²⁺ in different solvents

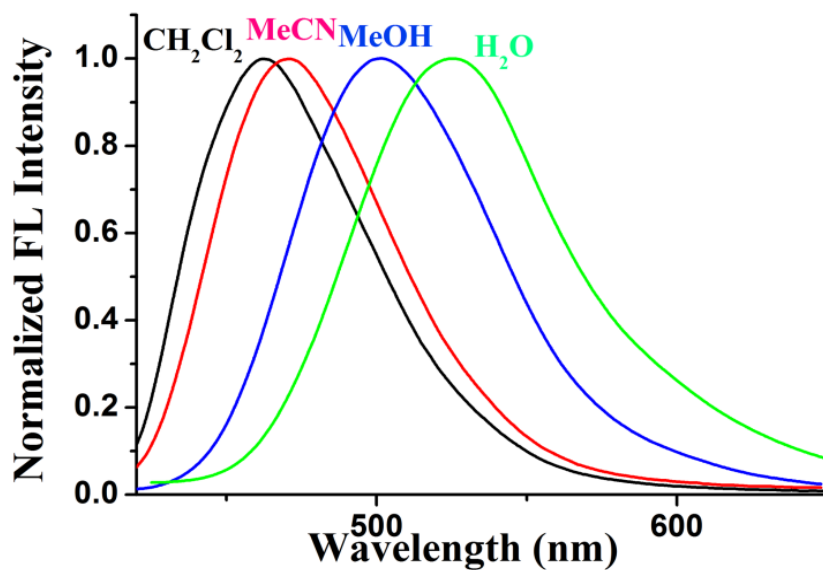


Figure S5. Emission spectra of BDAA/Hg²⁺ in different solvents

10. Calculated spatial distributions of HOMO and LUMO for BDAA

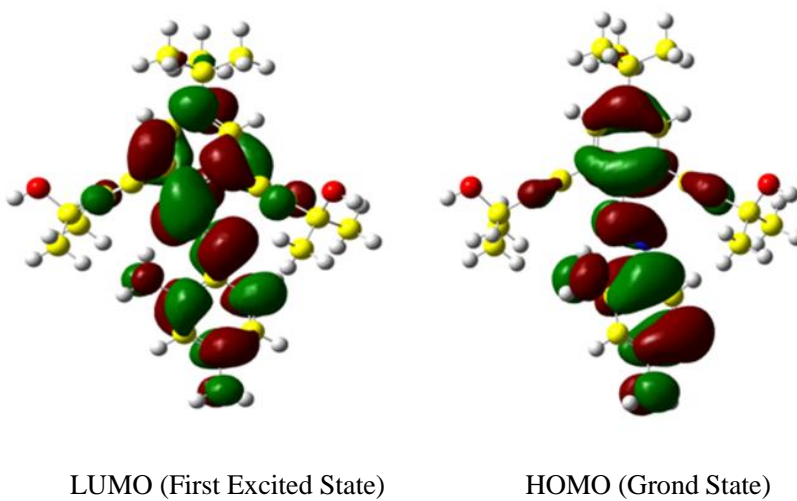


Figure S6. HOMO and LUMO of BDAA obtained by the B3LYP/6-31G method calculations.

11. Fluorescence enhancement with low concentration of Hg²⁺

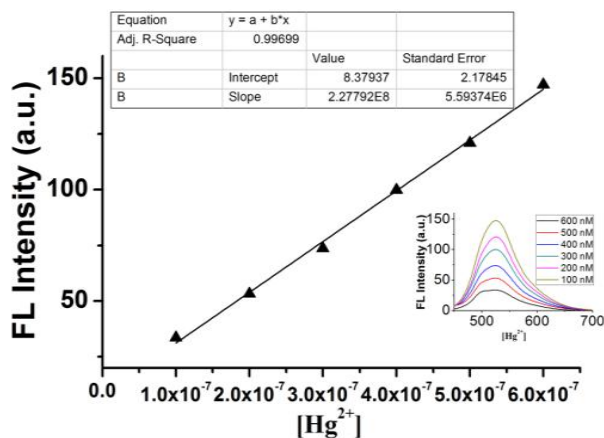


Figure S7. Fluorescence intensity of **BDAA** (10 μM) at 525 nm as a function of concentration of Hg^{2+} (100-600 nM) in HEPES buffer solution (50 mM, pH = 7.4). Inset: Emission spectra of **BDAA** in the presence of different concentrations of Hg^{2+} ion. Excitation and emission slit widths were 10 nm

12. Calculation of apparent association constant from fluorescence studies.

The association between the **BDAA** and Hg^{2+} ions was analyzed using the fluorescence data. The apparent association constant was calculated employing modified Benesi-Hildebrand method⁵ using Equation (2) where K is the association constant, I_0 is the fluorescence intensity of the free **BDAA**, I is the observed fluorescence intensity of the **BDAA**/ Hg^{2+} complex, and I_{max} is the fluorescence intensity at the saturation. The plot $1/(I-I_0)$ vs $1/[\text{Hg}^{2+}]$ gave a linear fitting, indicating a 1:1 stoichiometry between the **BDAA** and Hg^{2+} ions. The error for association constant estimated is < 10%.

$$\frac{1}{I-I_0} = \frac{1}{I_{\text{max}}-I_0} - \frac{1}{K(I_{\text{max}}-I_0)[\text{Hg}^{2+}]} \quad (2)$$

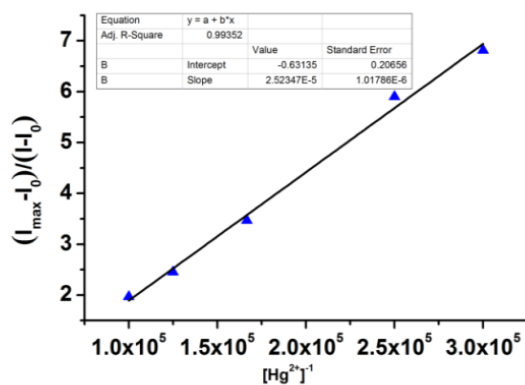


Figure S8. Benesi-Hildebrand plot for the determination of binding constant of Hg^{2+} with chemosensor **BDAA** in HEPES buffer solution (50 mM, pH = 7.4) at 25°C.

13. The reversibility of the sensor

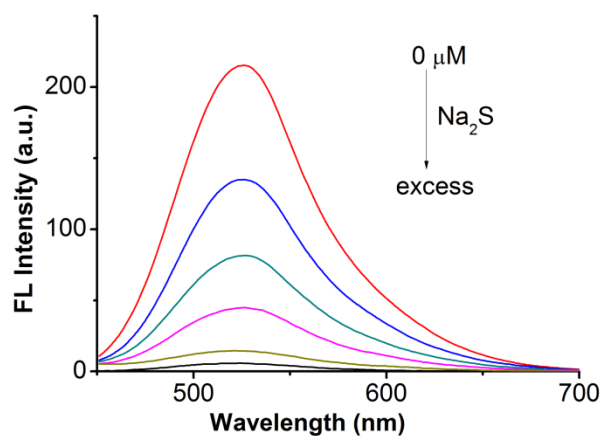


Figure S9 Emission spectra (excitation at 430 nm) of **BDAA** (10 μM) in the presence of Na_2S (0, 0.25, 0.5, 0.75, 1.0, 2.0 equiv). Excitation and emission slit widths were 3 and 6 nm, respectively.

14. ^1H NMR titration spectra

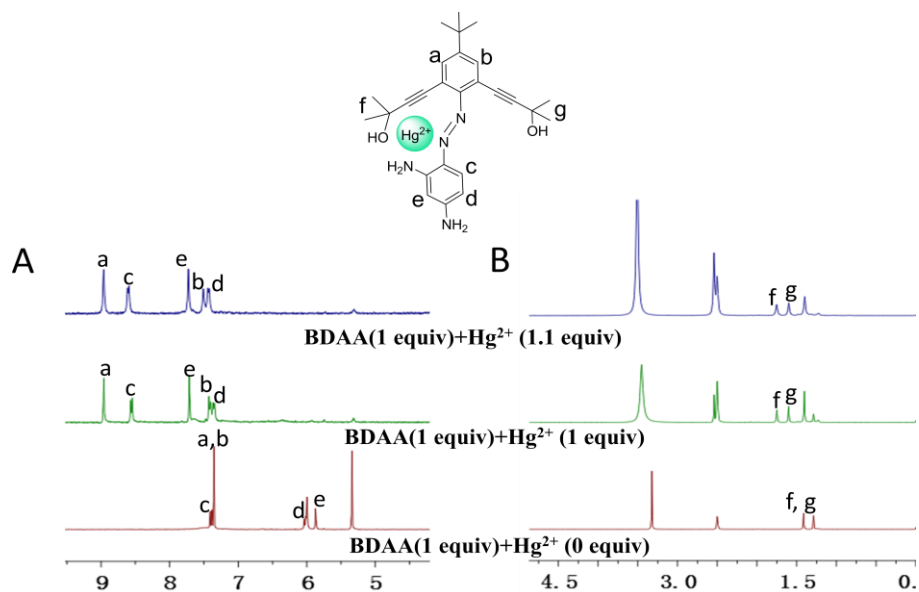


Figure S10. ^1H NMR spectra (A: aromatic region; B: aliphatic region) of sensor **BDAA** upon the addition of 0-1.1 equiv of Hg^{2+} in $(\text{DMSO})-d_6$.

15. 2D $^1\text{H}-^{13}\text{C}$ NMR spectra of the **BDAA** and **BDAA/ Hg^{2+}**

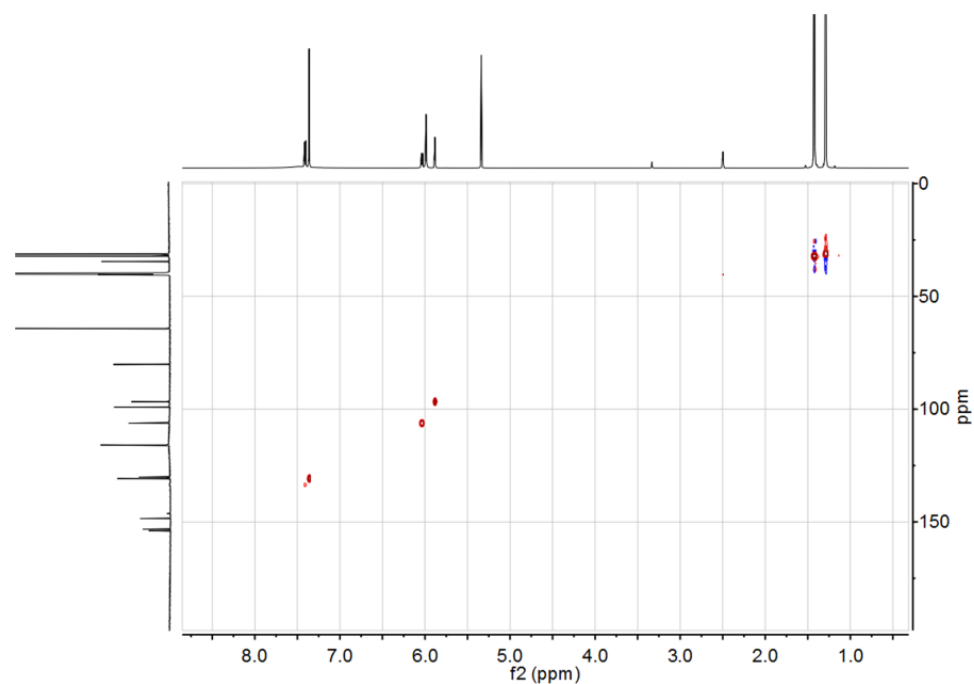


Figure S11. 2D $^1\text{H}-^{13}\text{C}$ HSQC spectrum of the **BDAA**

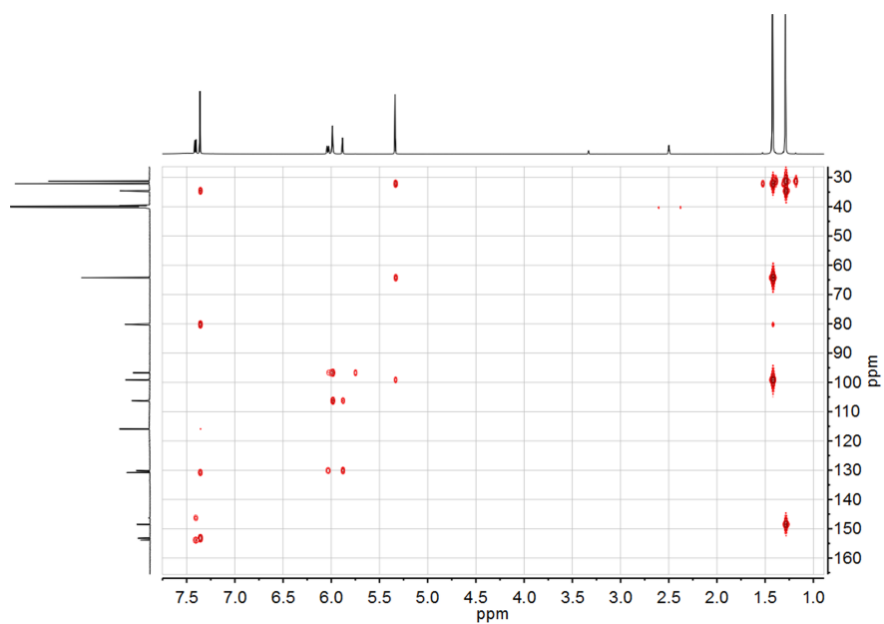


Figure S12. 2D ¹H-¹³C HMBC spectrum of the **BDAA**

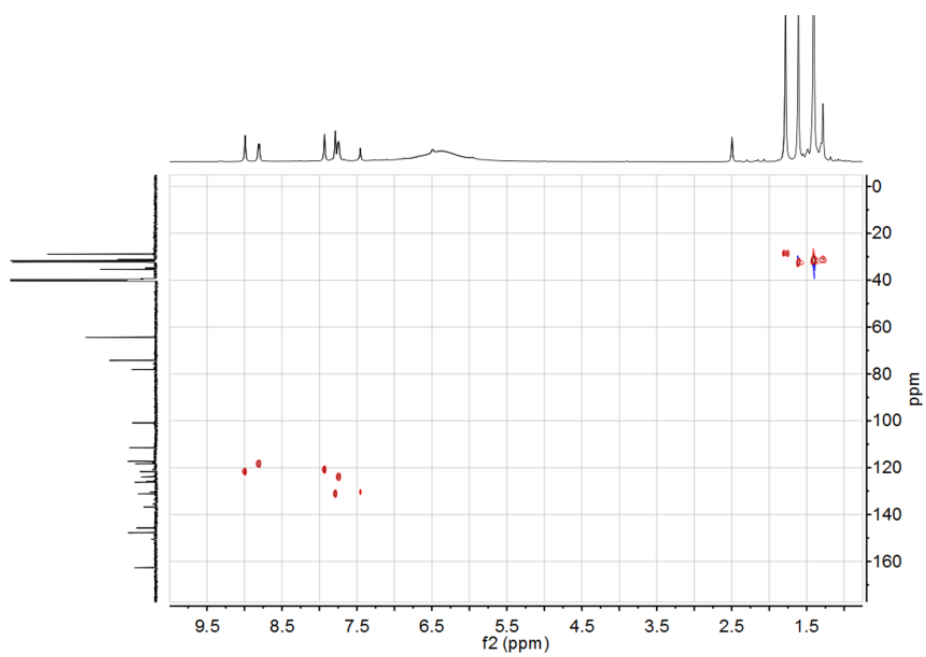


Figure S13. 2D ¹H-¹³C HSQC spectrum of the **BDAA+Hg²⁺**

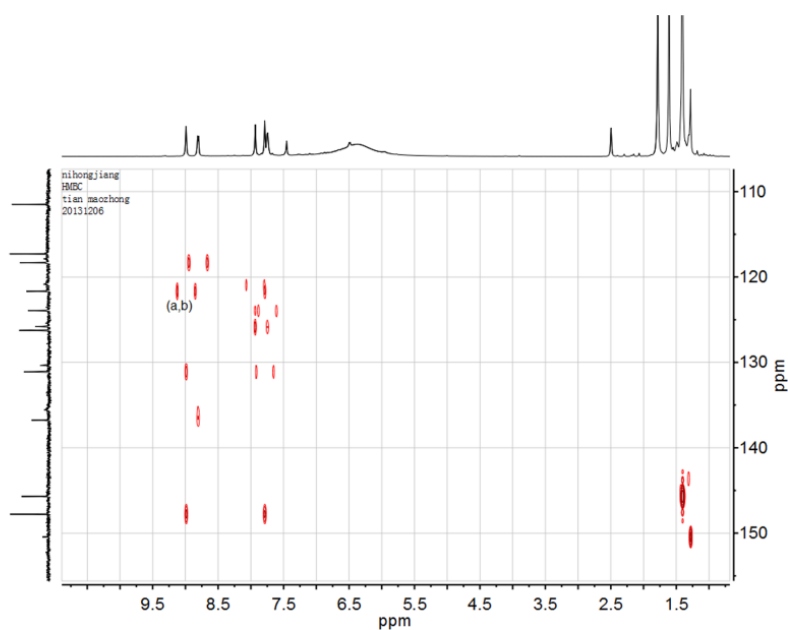


Figure S14. 2D ^1H - ^{13}C HMBC spectrum of the **BDAA+Hg²⁺**

16. Infrared spectra of the **BDAA** and **BDAA+Hg²⁺**

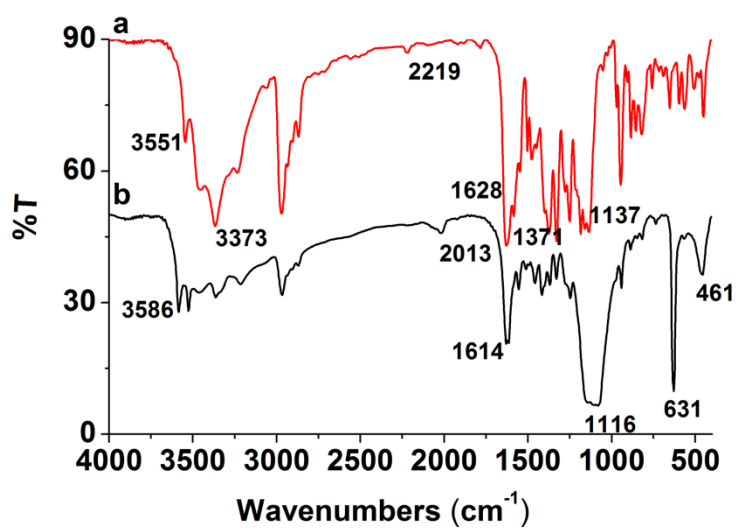


Figure S15. IR spectra of the **BDAA** and **BDAA+Hg²⁺**

17. MALDI-TOF mass spectrum of the **BDAA/Hg²⁺** complex

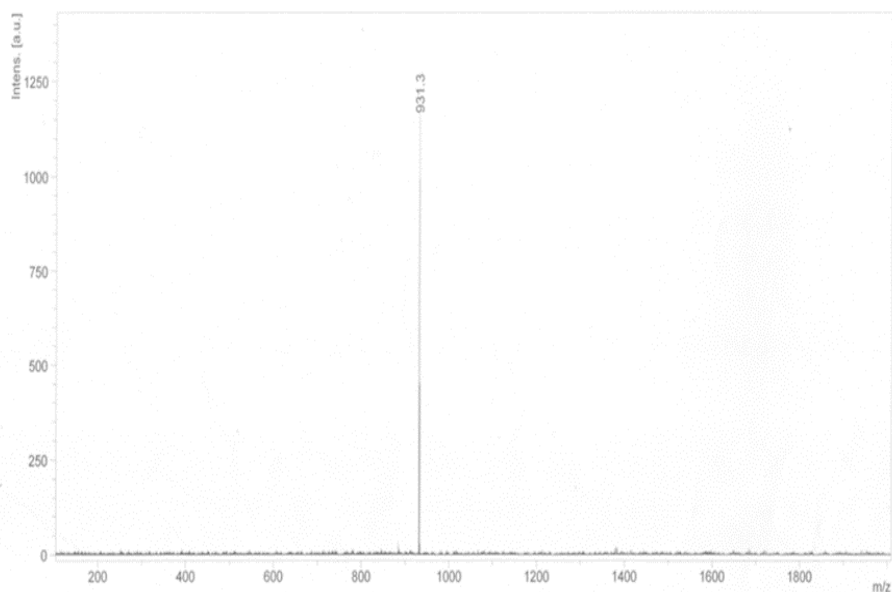


Figure S16. MALDI-TOF mass spectrum of the **BDAA**/ Hg^{2+} complex

18. Interfere of anions

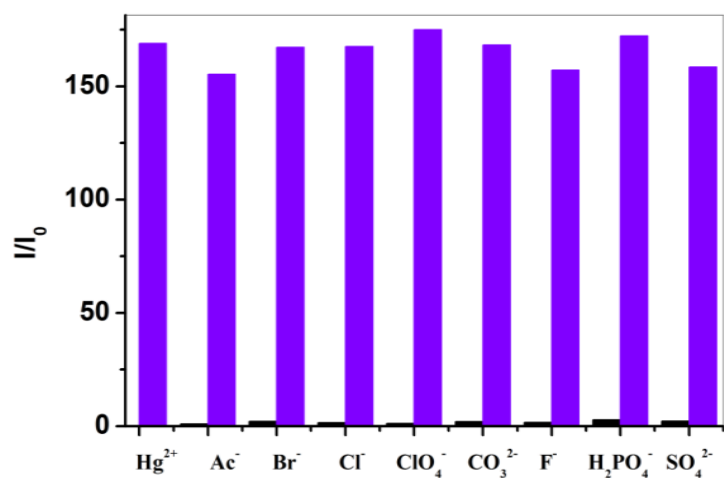


Figure S17. Histogram showing selectivity of **BDAA** (10 μM) for Hg^{2+} in HEPES buffer (50 mM, containing 0.1M KNO_3 , pH=7.4) solution. The black bars represent the I/I_0 value in the presence of various anions (10 equiv). The indigo bars indicate the change in the emission intensity upon subsequent addition of Hg^{2+} (3 equiv) to the solution containing **BDAA** and the anions of interest. For all measurements, $\lambda_{\text{exc}}=430$ nm; $T=298$ K. The signal intensity at $\lambda=525$ nm ($=I$) was normalized with that of the sensor-only sample ($=I_0$). Excitation and emission slit widths were 3

and 6 nm, respectively.

19. Confocal fluorescence images of live HT-29 cells with Hg^{2+}

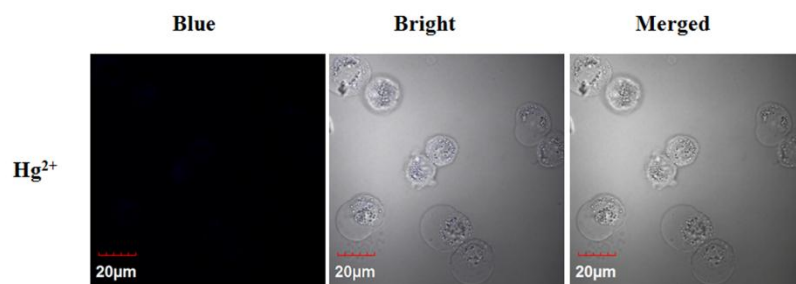


Figure S18. Confocal fluorescence images of live HT-29 cells incubated with 30 μM Hg^{2+} for 30 min.

20. The characterization data of sensor BDAA

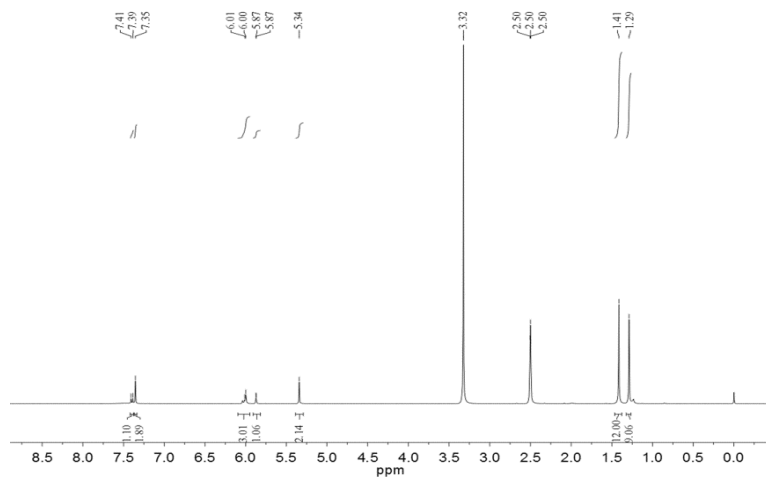


Figure S19. ^1H NMR spectra of BDAA in $\text{DMSO}-d_6$

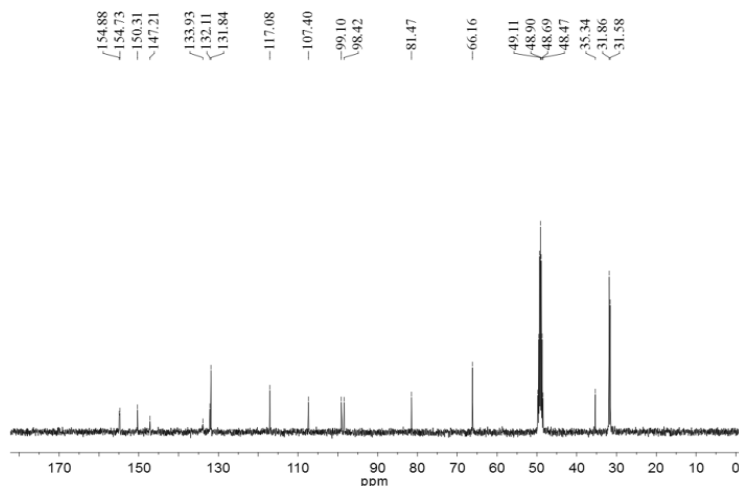


Figure S20. ^{13}C NMR spectra of BDAA in $\text{DMSO}-d_6$

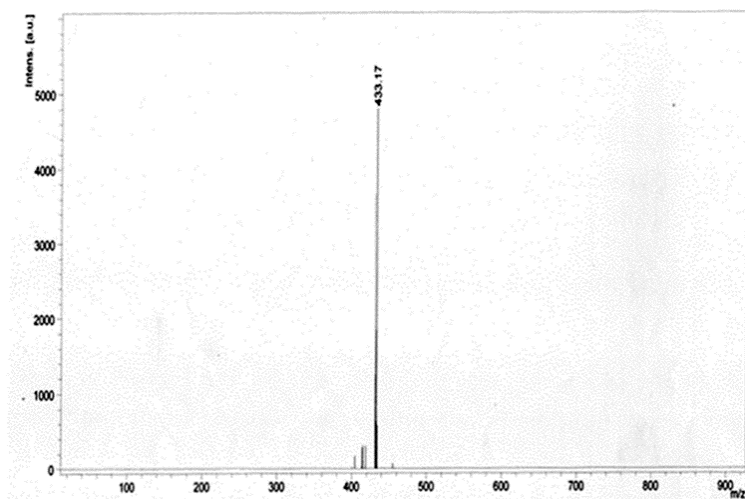


Figure S21. MALDI-TOF mass spectrum of the **BDAA**.

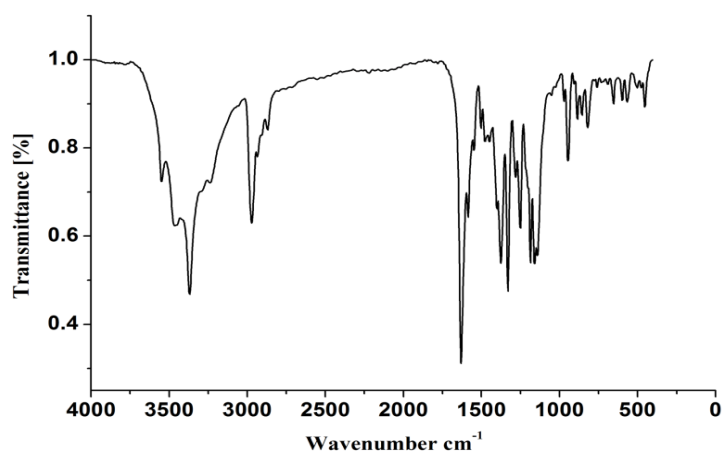


Figure S22. IR spectrum of sensor **BDAA**.

21. References

- 1 J. N. Demas, and G. A. Crosby, *J. Phys. Chem.*, 1971, **75**, 991.
- 2 N. J. Fitzmaurice, W. R. Jackson, and P. Perlmutter, *J. Organomet. Chem.*, 1985, **285**, 375.
- 3 H. Y. Lee, X. L. Song, H. Park, M. H. Baik, and D. Lee, *J. Am. Chem. Soc.*, 2010, **132**, 12133.
- 4 G. M. Sheldrick, SHELXS97 and SHELXL97, University of Gottingen, Germany, 1997.
- 5 H. A. Benesi, and J. H. Hildebrand, *J. Am. Chem. Soc.*, 1949, **71**, 2703.